



Engineering Hazard Evaluation of Active Faults and Research on the Method of Tunnel Anti-dislocation

B. Zhao⁽¹⁾, Z. Wang⁽²⁾

⁽¹⁾ Professor, Beijing Jiaotong University, bmzhao@bjtu.edu.cn

⁽²⁾ PhD Student, Beijing Jiaotong University, zjwang8911@hotmail.com

Abstract

In recent years, many investigations showed that underground constructions have suffered severe seismic damage during large earthquakes, and the tunnels intersected with active faults were one of the typical cases. Therefore, how to accurately ascertain the damage effects of dislocations and the way they act on the structures are the key issues for tunnel design and construction. First, based on the study of the 2008 Wenchuan earthquake, the destructive law between the tunnel damage degree and the distance towards active faults was established. We selected and defined some faults to be the “Engineering Faults”, meaning that they could cause direct damage to the engineering constructions. Next, aiming at the western area of China, we classified the fault types into strike-slip, dip-slip and strike-dip & dip-slip and established the regression relationships between the earthquake magnitudes and the fault parameters. Then, the structural behavior and the failure mechanism of the tunnels through targeted ruptures were analyzed by the numerical simulation method of the 3D geological model with dynamic finite element model. These established models could reflect the non-linear stress-strain features accurately since the analysis was shown to perform well to assess the tunnel behavior against severe seismic circumstance. Based on the results, the methodology for determining the anti-seismic joint and fortification design techniques were developed, which could take the flexibility and rigidity concept into consideration simultaneously and allow the underground constructions to have a better seismic resistance when passing the active faults. This paper provided a reference for the similar engineering constructions.

Keywords: tunnel damage; active fault; rupture parameters; through active fault; design method



1. Introduction

The geological conditions in the western China are complicated where the faults are of great activity. The macroseismic damage investigation indicated that active faults have caused great threats on tunnels and underground structures in areas of high seismic activity.

As for the preventive measures against different hazards of active faults, only the latest version of the Highway Engineering Seismic Code JTG-B02-2013 indicates a certain idea that if there is an active fault within the range of tunnel constructions, consideration should be paid for the influence of the seismogenic fault dislocation on the tunnel, thus special anti-seismic design for highway structure is required when it encounters the place where the peak ground acceleration is greater than or equal to 0.40g [1]. However, there is uncertainty in the current Seismic Code for the seismic design against active faults. Therefore, it is of great significance to develop the quantitative design methods of anti-dislocation for tunnel structures by analyzing the engineering hazards and evaluating rupture parameters of active faults.

The anti-dislocation combined joint is recognized as an effective anti-seismic measurement for tunnels through active faults, which can obviously reduce the longitudinal and lateral forces the tunnel suffers when fault dislocation occurs. The anti-dislocation combined joint had been applied for tunnels and underground constructions through active faults worldwide, for example: the Bolu tunnel in Turkey in 1999; the water tunnel of Koohrang-III in the central Iran; the New Monte Claire tunnel in California, United States in 2004, etc. However how to determine the fault rupture parameters in terms of different fault mechanisms and quantify the design of anti-dislocation combined joint for tunnel through active faults had not been investigated yet.

Therefore this paper summarized the tunnel damage types caused by active faults, analyzed the relationship between tunnel damage and active fault distance, proposed a potential evaluation method of active fault dislocations and studied the design method for setting anti-dislocation combined joint in tunnels. Since the actual deformation forms and sizes of active faults are very complicated [2, 3], how to determine appropriate deformation curve and value are the key points for the anti-dislocation design in tunnel engineering.

Specific contents included: firstly we summarized the correlations between tunnel damage type, level of tunnel damage with the distance towards active faults based on the investigation and analysis of the 2008 Ms 8.0 Wenchuan Earthquake; secondly by analyzing the 68 different cases of earthquake rupture in the western China, the correlations between earthquake magnitudes and rupture parameters were proposed and the regression relations were established; finally, according to the fault rupture parameters, we proposed a method of setting anti-dislocation combined joint for tunnels through different types of active faults.

2. Statistical Characteristics of Tunnel Seismic Damage in 2008 Wenchuan Earthquake

The survey focused on the 2008 Ms 8.0 Wenchuan earthquake, which collected and analyzed the seismic damage, thereby the destructive law between the tunnel damage degree and the distance towards active faults was established.

2.1 Tunnel Seismic Damage Type Classification

Based on the earthquake investigation, this paper divided the damaged tunnel into 15 types in terms of the earthquake damage phenomenon, damage degree of different tunnel components, which include: (1), lining cracks (cracks are clear with certain trends); (2), lining cracks (cracks are flaky or mesh without certain directions); (3), concrete spalling; (4), tunnel lining dislocation; (5), concrete blocks drop out; (6), secondary lining collapse; (7), tunnel collapse; (8), construction joint cracks; (9), lining seepage; (10), pavement cracks (cracks are clear with certain trends); (11), pavement cracks (cracks are flaky or mesh without certain directions); (12), inverted arch dislocation; (13), inverted arch uplift; (14), pavement seepage; (15), comprehensive seismic damage (consider all types of seismic damage together).

2.2 Tunnel Seismic Damage Degree Classification

According to the earthquakes effects on tunnels, the seismic damage degree was divided into four categories: severe disaster, medium disaster, slight disaster and no disaster and the corresponding damage type are shown in Table 1 while the histograms of tunnel disaster proportions regarding to the distance towards active faults are shown in Fig. 1.

Table 1 – Earthquake damage degree and damage types

Damage degree	Damage type
Severe disaster	tunnel lining dislocation, concrete blocks drop out, secondary lining collapse, tunnel collapse, inverted arch dislocation
Medium disaster	lining cracks (cracks are clear with certain trends), concrete spalling, inverted arch uplift
Slight disaster	lining cracks (cracks are flaky or mesh without certain directions), construction joint cracks, lining seepage, pavement cracks (cracks are flaky or mesh without certain directions), pavement seepage
No disaster	_____

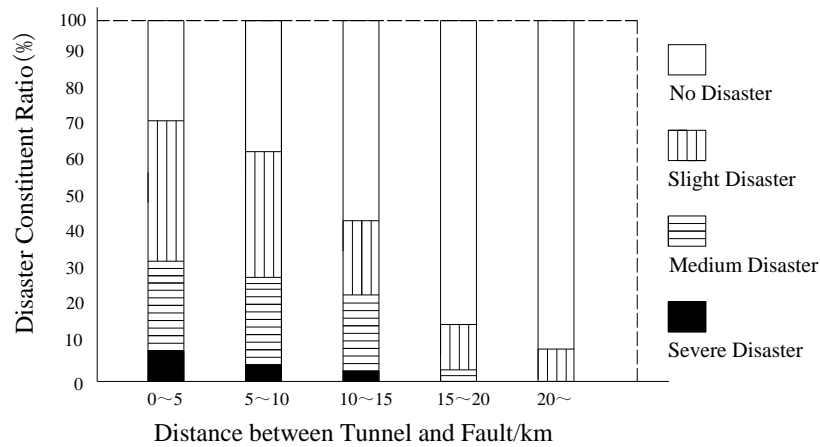


Fig. 1 – Relationship between damage degree and distance

Based on the research above, the relationship between tunnel damage and the distance towards the active faults can be summed as: the seismic damage was the worst from the fault zone within 5km and the degree was severe within 5-10km; meanwhile the damage degree was medium within 10-15km and slight when the distance was more than 20km. Therefore, when carrying out the anti-seismic engineering design, special attention should be paid for the type and degree of seismic damage from the fault zone within 10km. We defined such faults to be the “Engineering Faults”, meaning that they could cause direct damage to engineering constructions.

3. Evaluation of Fracture Parameters for Different Fault Types

Different causative fault features cause the rupture process of different characteristics, resulting in different rule that the seismic activity parameters and fracture parameters follow. Domestic and foreign researchers had carried out a number of researches, Wells and Coppersmith [4] established a famous guideline, where they sorted the faults by normal faults, reverse faults, strike-slip faults and unified the regression formula. Since determining the displacement index in the anti-seismic design for underground construction is of great importance, this paper examined the regression relationship of magnitude vs. displacement of reference [4] by the t test, however which showed a small significance of difference between normal faults and reverse faults, thus we grouped these two



types together as dip-slip faults. As for the other differences between normal and reverse faults, they can be dealt in the practical structural design. In addition, it is very common that faults are categorized as strike-slip and dip-slip type, therefore this paper investigated the statistical regressions by classifying the fault types into strike-slip, dip-slip and strike-slip & dip-slip.

3.1 Data and Analysis

This paper collected seismogenic fault activity parameters and fracture parameters of the 68 earthquakes in the western China from 1125 to 2013, including the Wenchuan earthquake, Yushu earthquake and Ya'an earthquake [5-7]. These earthquakes were classified according to the above standard and the investigated rupture parameters were magnitude (M_s), fracture length (L) and the maximum surface rupture displacement (D). We considered that since 1930 the earthquakes magnitudes were measured by the instruments, thus there were 44 events met this condition, whereas for older events, the magnitudes were derived from the literature review of the historical earthquake researches. Furthermore, the fracture lengths were available for 59 events while the maximum displacements were available for 60 events.

3.2 Regression Relationship between Magnitude and Rupture Parameters

There are several linear correlation expressions between the magnitude and rupture length as well as the maximum displacement, as follows [4]:

$$M_s = a + b \times \log(L) \quad \text{and} \quad \log(L) = a + b \times M_s \quad (1)$$

$$M_s = a + b \times \log(D) \quad \text{and} \quad \log(D) = a + b \times M_s \quad (2)$$

$$M_s = a + b \times \log(LD) \quad \text{and} \quad \log(LD) = a + b \times M_s \quad (3)$$

In the expressions, a and b are regression constants. Different fault types and different regions would obtain different statistical results. In this study, an assumption was made that the relationship between M_s and L was irrelevant to D ; the relationship between M_s and D was irrelevant to L ; when established the relationship between M_s and LD , the impacts from L and D on the magnitude were assumed to be the same.

The least square method was used to analyze the linear correlations of M_s vs. L , M_s vs. D and M_s vs. LD . The statistical regression results are shown in Table 2-4, the relationships are shown in Fig. 2-4, where the magnitudes recorded instrumentally are shown by solid symbols while those were derived from other data, by open symbols.

Table 2 – Earthquake magnitude vs. rupture length (L) regression

Fault types	Sample number	Regression by $M_s = a_1 + b_1 \log(L)$				Regression by $\log(L) = a_2 + b_2 M_s$			
		a_1 value	b_1 value	residual standard deviation	relative coefficient	a_2 value	b_2 value	residual standard deviation	relative coefficient
Strike-slip	34	4.83	1.4	0.38	0.917	-2.66	0.6	0.249	0.917
Strike-slip & dip-slip	22	4.01	1.85	0.67	0.9	-1.504	0.437	0.326	0.9
Dip-slip	12	4.18	1.95	0.48	0.744	-0.485	0.285	0.185	0.744
All	68	4.36	1.69	0.54	0.89	-1.743	0.469	0.285	0.89

Table 3 – Earthquake magnitude vs. the maximum displacement (D) regression

Fault types	Sample number	Regression by $M_s = a_1 + b_1 \log(D)$				Regression by $\log(D) = a_2 + b_2 M_s$			
		a_1 value	b_1 value	residual standard deviation	relative coefficient	a_2 value	b_2 value	residual standard deviation	relative coefficient
Strike-slip	34	6.399	1.402	0.524	0.85	-3.242	0.522	0.322	0.85
Strike-slip & dip-slip	22	6.69	1.41	0.339	0.975	-4.509	0.674	0.234	0.975
Dip-slip	12	7.09	1.005	0.327	0.848	-5.01	0.719	0.279	0.848
All	68	6.63	1.332	0.485	0.9	-3.977	0.608	0.329	0.9

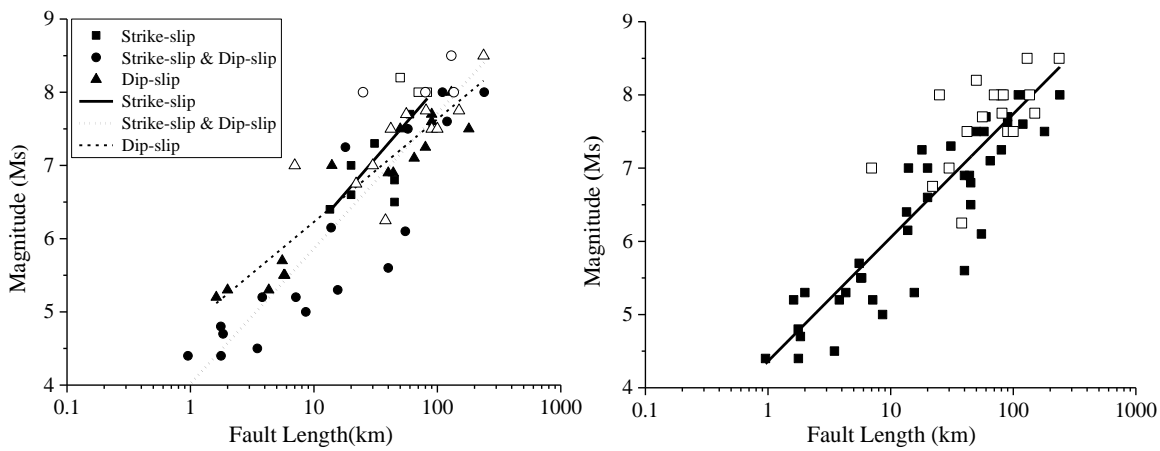


Fig. 2 – Magnitude vs. rupture length (L) regression.

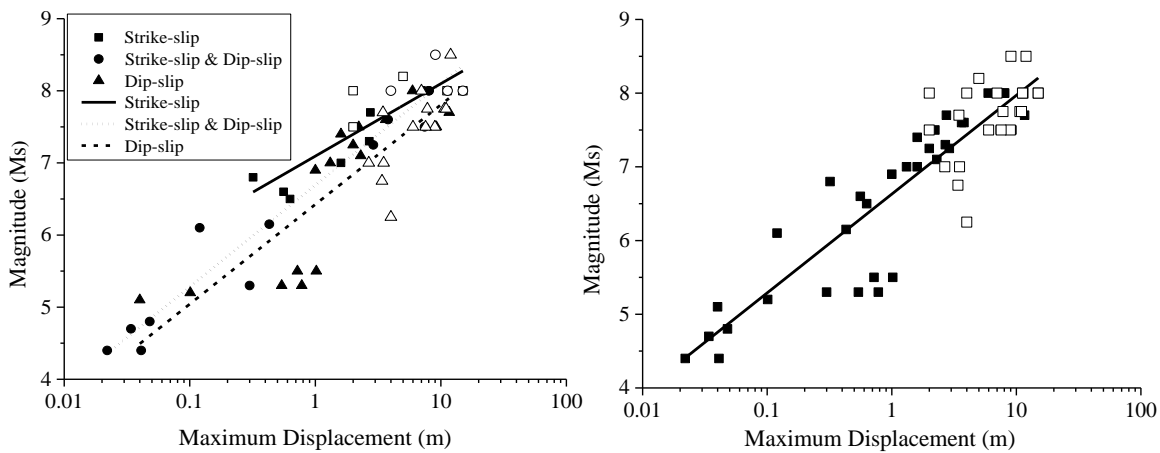


Fig. 3 – Magnitude vs. the maximum displacement (D) regression

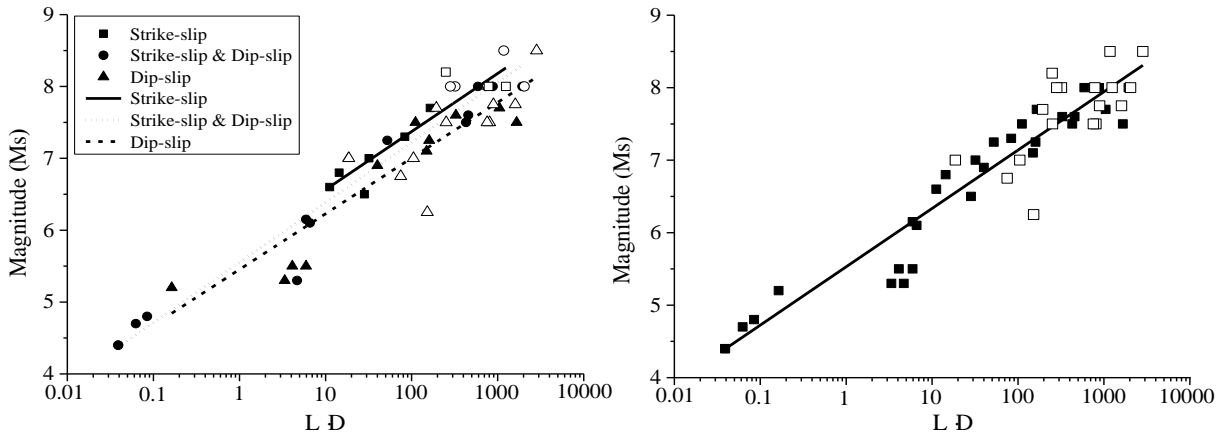


Fig. 4 – Magnitude vs. rupture length and the maximum displacement (LD) regression

Table 4 – Earthquake magnitude vs. rupture length and the maximum displacement (LD) regression

Fault types	Sample number	Regression by $M_s = a_1 + b_1 \log(LD)$				Regression by $\log(LD) = a_2 + b_2 M_s$			
		a_1 value	b_1 value	residual standard deviation	relative coefficient	a_2 value	b_2 value	residual standard deviation	relative coefficient
Strike-slip	34	5.454	0.775	0.4	0.899	-5.285	1.042	0.463	0.899
Strike-slip & dip-slip	22	5.55	0.835	0.311	0.979	-6.306	1.148	0.364	0.979
Dip-slip	12	5.755	0.809	0.281	0.915	-5.642	1.036	0.318	0.915
All	68	5.53	0.805	0.369	0.943	-5.909	1.106	0.433	0.943

4. Anti-Dislocation Combined Joint for Tunnel through Active Faults

Considering the relative rotation of the tunnel segments in the active fault, the seismic joint width should be preset. Therefore this paper established the design formulas of tunnel segment length for different fault width, dip angle and fault dislocation value, and the derived results were proved by the numerical simulation.

4.1 Anti-Dislocation Combined Joint

When the rupture occurs suddenly, the tunnel deformation failure mainly happens in the fracture zone or at the junction between the fracture zone and the host rock, the former is occurred in a narrow fault plane while the latter is for a wider fault plane. In both cases, we should obtain the deformation curve along the tunnel axial direction. As for the mountain tunnels, we analyzed the internal and surface deformation of rocks according to the method of Okada [8, 9] to be the deformation curve of the tunnel, since this method is an analytical solution, which cannot be used directly for constructions and interactions between rock and tunnel. Based on the obtained curve, a certain number of anti-dislocation combined joints could be set, allowing the tunnel to be divided into several inter cells where the structure connections become flexible. Thus the tunnel sections were relatively independent on both sides of the fracture zone and the deformation caused by the fault slip would be absorbed by these flexible connections, leading the whole force of the tunnel structure to be released. In addition, for larger deformations, our proposed method can combine the approach of enlarging the tunnel diameter (over-excavation) to resist the deformation and keep the tunnel to be relatively flat.

4.2 Design Method for Tunnel through Fault Zone

4.2.1 Computational Derivation Hypothesis

According to the previous researches, when tunnel passes through a narrow fault zone, the joint opening amount is the maximum at the junction between fault zone and host rock and there is no relative rotation in the lining on both sides of the anti-dislocation combined joint. In order to ensure that the tunnel would not damage, the following assumptions should be made before the calculations:

- (1) Assuming that there is no dislocation in each tunnel segment within the fault zone core, the dislocation generated by the surrounding rock is digested by the relative rotation angle of the adjacent sections;
- (2) Assuming that there is no relative rotation angle between each tunnel segment except for the fault zone core part;
- (3) Due to the rotation angle of the tunnel segment is relatively small, assuming that the change of the rotation angle in the adjacent anti-dislocation combined joint is linear.

4.2.2 Computational Derivation

The calculation process is shown in Fig. 5, where W is the fault fracture zone width, h is the tunnel height, $2d$ is the fault vertical displacement, β is the fault dip angle, r is the preset width of the anti-dislocation combined joint, θ is the absolute rotation angle of the adjacent two lining segments which have no relative rotation in the middle of tunnel, and α is the maximum opening amount of the anti-dislocation combined joint in the tunnel at the fault fracture zone.

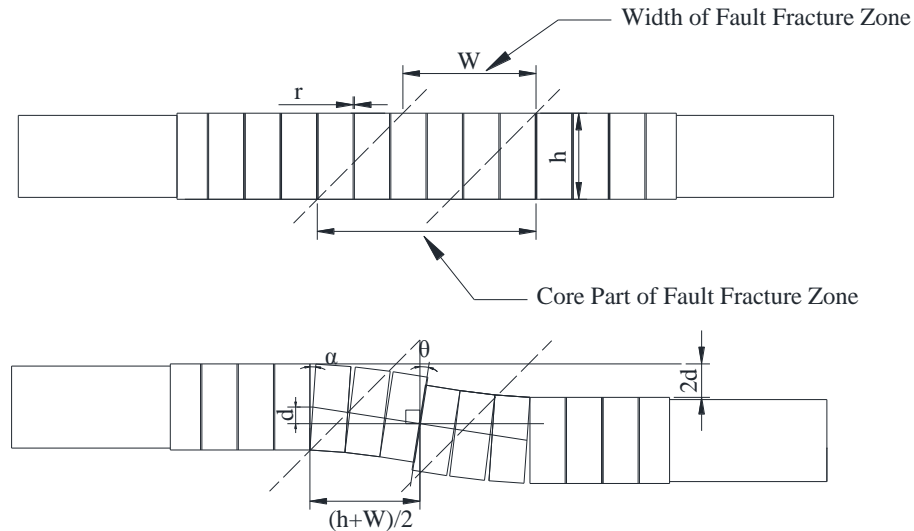


Fig. 5 – Before and after the deformation of tunnel secondary lining

Because of the fault dislocation, the rotation angle θ of the anti-dislocation combined joint in the middle of the longitudinal tunnel is:

$$\theta = \frac{d}{\frac{W+h\cot\beta}{2}} = \frac{2d}{W+h\cot\beta} \quad (4)$$

When the relative maximum rotation of the two adjacent sections of the tunnel occurs, the maximum relative rotation angle α of the preset anti dislocation combined joint is:

$$\alpha = \frac{r}{h} \quad (5)$$



According to the hypothesis (1), the total rotation angle θ of the dislocation is born by the relative rotation angle of the two adjacent segments. And according to the hypothesis (3), by the summation formula of arithmetic progression:

$$\theta = \frac{n}{2}(0 + \alpha) \quad (6)$$

where

$$n = \frac{2\theta}{\alpha} = \frac{2 \frac{2d}{W+h\cot\beta}}{\frac{r}{h}} = \frac{4dh}{r(W+h\cot\beta)} \quad (7)$$

n is the minimum number of cycles required from the edge of core part of fault fracture zone to the tunnel longitudinal axis. According to the above formulas:

$$N = 2n = \frac{8dh}{r(W+h\cot\beta)} \quad (8)$$

N is the minimum number of segments that need to be set when the tunnel passes through the active fault. If N is not an integer, take the value of N' to be an integer greater than N .

Thus under the premise that the tunnel is not damaged, the maximum segment length of the tunnel through the active fault is:

$$a = \frac{W+h\cot\beta}{N'} \quad (9)$$

4.3 Numerical Simulation Verification

4.3.1 Model and Parameters

Three numerical models were established to verify the performance of the anti-dislocation combined joint. The parameters were set as fault dip is 45°, surrounding rock grade is IV and fault zone width is 50m. The mechanical properties of the materials are summarized in Table 5. We did not set any seismic measures for A model, while B model was set with the joint for every 15m per lining segment, and the joint width was 10cm. Based on the method determined by Constantopoulos [10], C model was applied according to the optimization algorithm proposed by this paper: set the joint of every 5m for tunnel lining where the rock properties change and set 10m in the remaining parts, the joint width was 10cm.

The length of the model was 200m, the width was 120m, the height was 100m, and the tunnel was located in the center of the model. The fault width was 50m, the fault dislocation was 0.8m, the fortification area length for tunnel was 100m. The rock, fracture zone and the initial lining were simulated by solid elements, the secondary lining was simulated by 3D shell element. The lining adopted the concrete damage constitutive model and the surrounding rock and fault fracture zone adopted the Drucker-Prager constitutive relation. The parameters of rock, soil layer and joint material are in Table 5 and the above three tunnel models are shown in Fig. 6.

Table 5 – Physical parameters for calculation

Metrials	Elasticity modulus (Gpa)	Poisson ratio (/)	Unit weight (KN/m ³)	Frictional angle (°)	Cohesion (Gpa)
Surrounding rock	3	0.28	24	45	1.2
Fault fracture zone	1	0.35	18	30	0.25
Primary lining	30	0.2	22	—	—
Secondary lining	31.5	0.2	25	—	—
Material of joints	0.001	0.38	20	—	—

4.3.2 Results of Simulation

The most dangerous secondary lining section was chosen from these three models, and 8 characteristic positions from each section were selected to analyze and study the transverse internal force of the tunnel. The data was selected by every 0.5m to investigate the secondary linings' longitudinal bending moment at the invert. The calculation results are shown in Fig. 6-10.

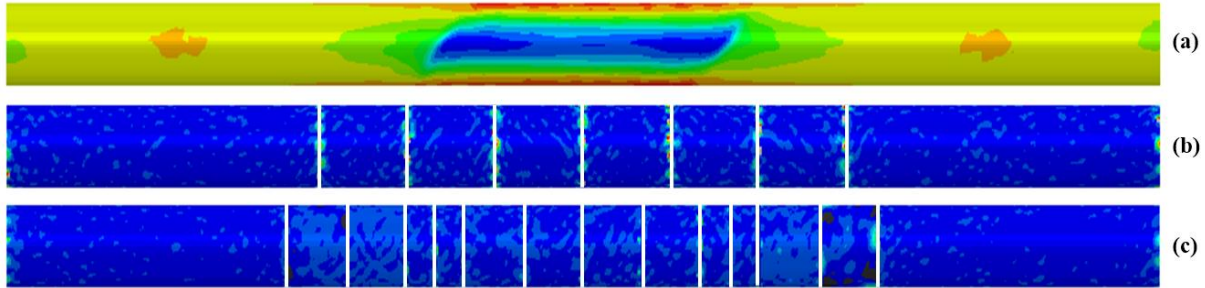


Fig. 6 – An example of the simulation results (longitudinal bending moment) of the three models.

(a) Result of A model; (b) Result of B model; (c) Result of C model

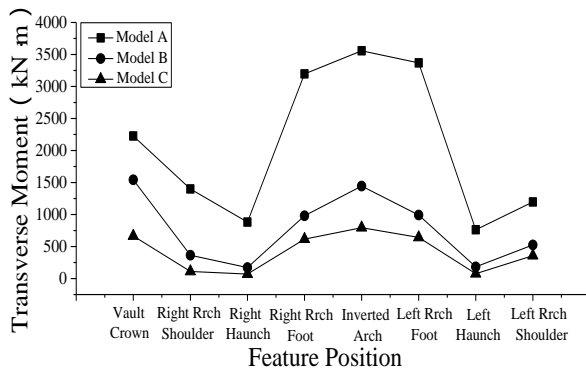


Fig. 7 – Transverse moment of the secondary linings

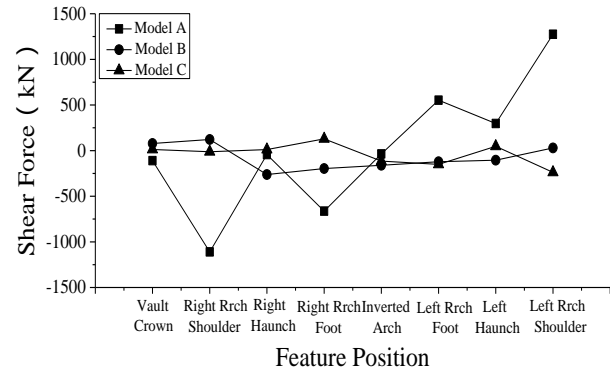


Fig. 8 – Shearing force of the secondary linings

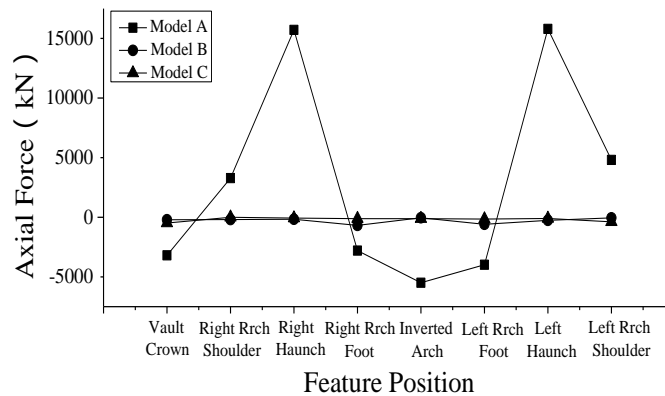


Fig. 9 – Axial force of the secondary linings

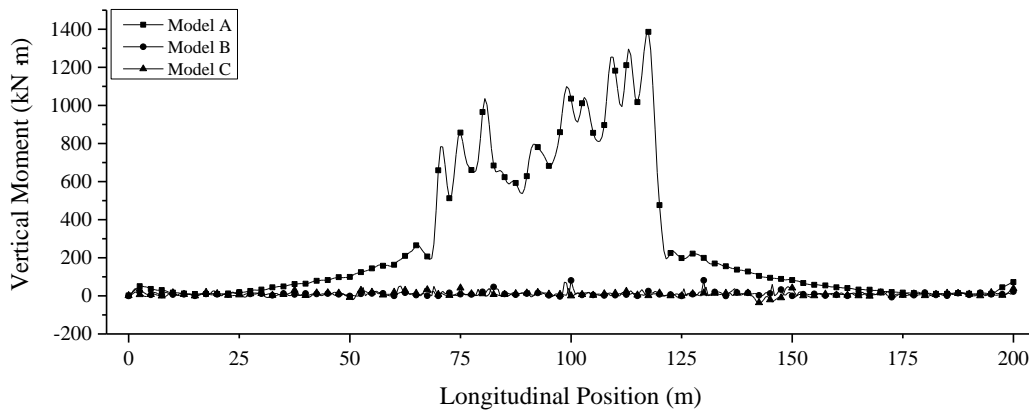


Fig. 10 – Longitudinal bending moment of the secondary linings

The analysis of the numerical simulation results:

(a) The transverse bending moment of the most dangerous section of model A was greater than that of the model B and model C, the transverse moment of model C was the smallest; (b) The axial force and shearing force of the most dangerous section of model A were greater than those of model B and model C, the axial force and shearing force of model C were slightly less than those of model B; (c) The longitudinal bending moment of model A was much larger than that of model B and model C. In the fault core and its periphery, the longitudinal bending moment of model A was larger than the other sections of the tunnel, but the longitudinal moment of model B and model C was not changing obviously along the tunnel. The maximum longitudinal bending moment of model C was smaller than that of model B.

5. Conclusion and Prospect

In this paper, the engineering hazards of active faults were analyzed and the relationships between magnitude and seismic rupture parameters corresponding to different active fault mechanism were established. According to the requirements of tunnel through active faults, deformation characteristics of surrounding rock were evaluated, the quantitative design method of the anti-dislocation combined joint in the tunnel structure through different active faults was proposed. The main conclusions were obtained as follows:

(1) Based on the seismic hazard analysis of the 2008 Wenchuan earthquake, the seismic damage of tunnels and the distance towards the main fault zone were divided into different classifications, the types of earthquake disaster were classified and statistically analyzed. The tunnel damage degree with different fault distance were summarized.

(2) Aiming at the 68 different earthquakes in the western China, the fault was classified into strike-slip, dip-slip and strike-slip & dip-slip; by analyzing the magnitudes, seismic rupture length and the maximum surface rupture displacement, the regression relationships between the earthquake magnitude and rupture parameters of different fault types were established where the proposed indexes were found to be more reasonable.

(3) This paper evaluated the soil deformation characteristics within a wide fracture zone, and proposed the methods of setting anti-dislocation joint when tunnels pass through different faults, the validity of which were verified by the 3D numerical simulation, providing a basis for the design of the tunnel through active faults.

Considering the relevance between active faults and tunnel engineering, the potential hazards of active fault motions on tunnel engineering could be evaluated; based on quantifying the dislocations at ground surface and fault plane, the dislocation of the tunnel could be derived; according to the active fault parameters at the engineering location, the earthquake seismic measures could be taken. The above three results provided a theoretical reference for the engineering design of tunnels pass and/or near active faults.



6. Acknowledgements

This research has been supported by the National Natural Science Foundation of China (No.U1434210, No.51278045 and No.40674016), the Science and Technology Promotion Project of China Ministry of Railway (No. 2010G018-C-1), the Project of Shenzhen Metro Group Co., Ltd (No. SZ-CGM-KY001/2014). We are grateful to Prof. A.L. Strom who read the manuscript and offered useful comments and suggestions.

7. References

- [1] JTG B02-2013 (2013): Specification of seismic design for highway engineering, Beijing: China Communication (in Chinese).
- [2] Strom AL, Nikonov AA (1997): Relationship between the seismogenic fault parameters and earthquake magnitude. *Izvestiya Physics of the Solid Earth*, **33** (12), 1011-1022.
- [3] Strom AL, Nikonov AA (2000): The distribution of slip along seismogenic faults and incorporation of nonuniform slip in paleoseismological research. *Volc. Seis.*, **2**, 705-722.
- [4] Wells DL, Coppersmith KJ (1994): New empirical relationships among magnitude, rupture length, rupture width, rupture area, and surface displacement. *Bulletin of the Seismological Society of America*, **84** (4), 974-1002.
- [5] Wu Z, Yuan Y (1990): Surface ruptures and seismogenic faults. *Journal of Catastrophology*, **4**, 14-19 (in Chinese).
- [6] Deng Q, Zhang P, and et al (2003): Active tectonics and earthquake activities in China. *Earth Science Frontiers*, **10**, 67-73 (in Chinese).
- [7] Pan J, Li H, and et al (2011): Surface rupture characteristics, rupture mechanics, and rupture process of the Yushu Earthquake (Ms7.1). *Acta Petrologica Sinica*, **27** (11), 3449-3459 (in Chinese).
- [8] Okada Y (1985): Surface deformation due to shear and tensile faults in a half-space. *Bulletin of the Seismological Society of America*, **75**, 1135-1054.
- [9] Okada Y (1992): Internal deformation due to shear and tensile faults in a half-space. *Bulletin of the Seismological Society of America*, **82**, 1018-1040.
- [10] Constantopoulos JV (1981): The dynamic analysis of the tunnel. *Modern Tunneling Technology*, **1**.